Published by
NIGERIAN SOCIETY OF PHYSICAL SCIENCES
Available online @ https://journal.nsps.org.ng/index.php/jnsps

J. Nig. Soc. Phys. Sci. 6 (2024) 1970

Journal of the Nigerian Society of Physical Sciences

Stagnation point flow of viscous nanofluid towards a shrinking sheet with quadratic buoyancy and thermophoresis influence: convection through porous media

J. U. Abubakar[a], T. L. Oyekunle[a], M. T. Akolade[b], S. A. Agunbiade[c,*]

[a]Department of Mathematics, University of Ilorin, Ilorin, Nigeria
[b]Department of Computer Science, Lead City University, Ibadan, Nigeria
[c]Department of Basic Sciences, Babcock University, Ogun State, Nigeria

Abstract

This study investigates the dynamics of heat and mass transfer, focusing on the impact of nonlinear convection and thermophoresis in the flow of viscous nanofluid towards a shrinking sheet embedded with a porous matrix. To facilitate understanding of the flow behavior, the study employs similarity variables to simplify the resulting nonlinear partial differential equations. Numerical analysis utilizing the collocation method with Legendre polynomials as basis functions reveals distinct distributions of velocity, temperature, and concentration. The results demonstrate that the dimensionless suction coefficient amplifies nanoparticle volume fraction and momentum along the stretching surface. In addition, an increase in internal frictional force leads to heightened injection of heat energy, accelerates the temperature field, and impedes nanoparticle diffusion due to heat absorption. Elevation of convection terms augments momentum, reduces energy dispersion, and enhances nanoparticle diffusion. Moreover, an increase in the dimensionless Eckert number (Ec) correlates with intensified energy and diminished diffusion concentration of the nanoparticle volume fraction.

DOI:10.46481/jnsps.2024.1970

Keywords: Nonlinear convection, Nanofluid, Thermophoresis, Darcy law, Stagnation point

Article History :
Received: 14 January 2024
Received in revised form: 26 May 2024
Accepted for publication: 30 May 2024
Published: 07 July 2024

Communicated by: J. Ndam

1. Introduction

The phenomenon of fluid convection, where a gas or liquid comes to a rest at a specific location, is commonly known as stagnation point flow. This behavior is characterized by the convergence of fluid particles around an object, resulting in zero velocity. The analysis of fluid dynamics around stagnation points is crucial in engineering applications, offering valuable insights into pressure distributions, lift, and drag forces, particularly in aerodynamic and hydrodynamic contexts [1–3]. Physically, applications of this phenomenon are found in various fields, such as heat exchangers or thermal systems.

Numerous researchers have contributed to the comprehensive assessment of stagnation point dynamics across different disciplines. Setting the record straight, Brimmo and Qasaimeh

*Corresponding author: Tel.: +234-816-995-3938
Email addresses: abubakar.ju@unilorin.edu.ng (J. U. Abubakar), tloyekunle95@gmail.com (T. L. Oyekunle), akolade.mojeed@lcu.edu.ng (M. T. Akolade), agunbiades@babcock.edu.ng (S. A. Agunbiade)

[4] critically analyzed these dynamics in life sciences and analytical chemistry, while Khashiie *et al*. [5] incorporated the injection of hybrid nanofluids in mathematical modeling for simulating flow past a Riga surface. Makinde *et al*. [6] investigated radiative heat transfer and slip impact for stagnation point flow toward a stretchable convective surface. Shahid [7] highlighted the response of mass diffusion, thermophoresis, and Brownian motion in a magnetized Upper-Convected Maxwell (UCM) fluid. Recent studies encompass the analysis of buoyancy features over a spinning sphere by Zaheer *et al*. [8], Kenea and Ibrahim [9] exploration of non-Fickian and non-Fourier flux conditions in rotating systems, and Awati *et al*. [10] utilization of spectral and Haar wavelet collocation methods while enumerating the viscous dissipation effect on micropolar nanofluid, among others.

The industries, fields of science and engineering consider applications of nonlinear convection particularly important in processes requiring high temperatures, as emphasized by Patil and Kulkarni [11]. It's impact on flow processes has been extensively studied by researchers such as Raju *et al*. [12] and Raju *et al*. [13], where investigation encompassing nonlinear convection with time dependency and quadratic convection through a Darcy porous medium is analyzed. Their findings indicate an increase in fluid particle momentum with quadratic convection. An investigation of heat and mass transfer enhancement by Khan *et al*. [14] presented the Buongiorno model of nanofluid nonlinear mixed convection with melting heat phenomenon. Their findings reveal that the fluid nanoparticle concentration decreases for melting response and entropy generation enhancement is observed for melting and magnetic variables. Akolade *et al*. [15, 16] with the study of Carreau fluid and Williamson fluid respectively discussed the concept of nonlinear convection via different numerical scheme. Further analysis of nonlinear convection in various geometries includes the study of Casson fluid flow through an annular micro-channel by Idowu *et al*. [17], investigation of multi-slip and Soret-Dufour effects over a nonlinear slendering sheet by Olabode *et al*. [18], and exploration of a shrinking sheet investigation towards stagnation point flow by Kumar and Sood [19]. Furthermore, Pati and Shankar [20] analysis on the influence of activation energy in a double-diffusive dusty fluid flow over a cone, among other geometries. Across these findings, it is consistently observed that fluid velocity increases with nonlinear convection.

The flow of fluid over a stretching surface and porous media presents classic challenges in fluid dynamics with diverse industrial and natural applications. In industries such as printing, paper, and textile manufacturing, the process of coating and film deposition often involves the flow of fluids over stretching surfaces. Moreover, understanding the dynamics of porous media is crucial for achieving wide range of applications such as thermal energy storage, geothermal energy utilization, petroleum reservoirs, storage of grain, buried electrical cables etc. Consequently, the effects of permeability of the porous medium when the flow is characterised by Darcy's law was theoretically investigated recently in different geometry and based fluid assumptions. Alam *et al*. [21] and Agunbiade *et al*. [22] examined stretching porous media with nanofluids, Prandtl nanofluidic flow via a stretching sheet was examined by Ramanjini *et al*. [23]. In a related study, Deba *et al*. [24] and Goud *et al*. [25] presented their investigations on the dynamics of Williamson fluid. Combined effects of thermosolutal convection in Jeffery Nanofluid with porous medium was investigated by Lata *et al*. [26], where the impact of magnetic field response was identified. Sharma *et al*. [27] and [28] studied the energy instability, variable gravity and magnetic field influence of Jeffery nanofluids via porous media. An investigation on the onset of convection with extended Darcy-Forchheimer law was presented by Yadav *et al*. [29], a similar study by Yadav [30] analyzed the convection with heat-generating effect for Jeffery fluid all in porous medium while Yadav *et al*. [31] recent study explores the double diffusive convection in porous membrane enclosures soaked with Maxwell fluid. Moreover, recent study of Sharma *et al*. [32] incorporates the specific effects of the electric field, Brownian motion, thermophoresis, and rheological factors, with critical analysis of the porous matrix response being enumerated. In a related study, Sharma *et al*. [33] identify the rotation effect and the thermal instability of Jeffrey nanofluids with variable gravity.

Inspired by previous studies, the current study aims to explore the combined influence of thermophoresis, Darcy and viscous dissipation, and nonlinear convection on stagnation point flow of viscous nanofluid towards a shrinking sheet. To the authors' best knowledge, a combined investigation of this kind is presented for the first time. The analysis of velocity, temperature, and concentration profiles in response to variations in pertinent parameters is conducted through an approximate numerical approach using Legendre polynomials as basis functions and the collocation technique.

2. Problem formulation

The geometry depicted in Figure 1 illustrates the Cartesian coordinate system used to represent the considered porous incompressible viscous fluid. This system facilitates the analysis of two-dimensional steady convection flow directed towards a shrinking surface. The x-axis, perpendicular to both the y-axis and the sheet, remains parallel to the latter, maintaining a fixed origin. In this setup, the velocity of the external fluid is denoted as $\mathrm{U_e} = \mathrm{ax}$, while $\mathrm{U_w} = \mathrm{cx}$ represents the velocity of the sheet. Here, $a > 0$ signifies the constant strength of the stagnation flow, and $c > 0$ denotes the constant stretching of the sheet. Additionally, the temperature and concentration of the shrinking sheet are expressed as $\mathrm{T} = \mathrm{T_w}(\mathrm{x})$ and $\mathrm{C} = \mathrm{C_w}(\mathrm{x})$, respectively. The ambient temperature is designated as $\mathrm{T} = \mathrm{T_\infty}$, while the ambient concentration is represented as $\mathrm{C} = \mathrm{C_\infty}$.

The flow governing equations based on the above assumption and following the work of Kumar and Sood [19], Japili *et al*. [34], and Rakesh and Shilpa [35] are taken as follows:
Equation of continuity:

$$\frac{\partial u}{\partial x} + \frac{\partial v}{\partial y} = 0, \tag{1}$$

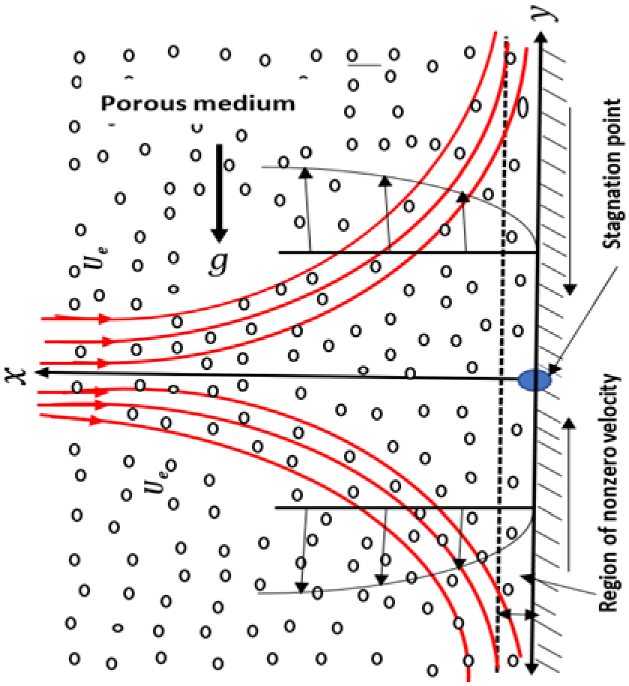

Figure 1: Stagnation point flow model configuration with Darcy dissipation.

Equation of momentum:

$$\left.\begin{array}{l} u\,\frac{\partial u}{\partial x}+v\,\frac{\partial u}{\partial y}=U_e\frac{\partial U_e}{\partial x}+v\,\frac{\partial^2 u}{\partial y^2}+\frac{\nu_f}{K}\left(U_e-u\right)\\ +\,g\beta_0\,\left(T-T_\infty\right)+\,g\beta_1\,\left(T-T_\infty\right)^2\\ +\,g\beta_2\left(C-C_\infty\right)+\,g\beta_3\left(C-C_\infty\right)^2 \end{array}\right\}. \quad (2)$$

Equation of energy:

$$\left.\begin{array}{l} u\,\frac{\partial T}{\partial x}+v\,\frac{\partial T}{\partial y}=\alpha\,\frac{\partial^2 T}{\partial y^2}+\tau\left[D_B\frac{\partial C}{\partial y}\frac{\partial T}{\partial y}+\frac{DT}{T_\infty}\left(\frac{\partial T}{\partial y}\right)^2\right]\\ +\,\frac{Q_1}{\rho C_p}\left(T-T_\infty\right)+\frac{\mu_f}{\rho C_p}\left(\frac{\partial u}{\partial y}\right)^2+\frac{\mu_f}{\rho C_p K}\left(U_e-u\right)^2, \end{array}\right\}.(3)$$

Equation of concentration

$$u\,\frac{\partial C}{\partial x}+v\,\frac{\partial C}{\partial y}=D_B\,\frac{\partial^2 C}{\partial y^2}+\frac{DT}{T_\infty}\,\frac{\partial^2 T}{\partial y^2}. \quad (4)$$

The assumed boundary conditions for the model equations takes:

$$\begin{array}{l} v=0,\;u=cx,\;T=T_{\mathrm{w}}=T_\infty+bx,\\ C=C_w=C_\infty+dx \text{ at } y=0, \end{array} \quad (5)$$

$$u\;\rightarrow U_e\left(x\right)=\;ax,\;\;T\rightarrow T_\infty\;\text{ and } C\rightarrow C_\infty\;\text{ as }\;y\rightarrow\infty. \quad (6)$$

Equations (1) - (6) are transformed into the following non-linear differential equations, using the stream function and similarity transformation variables. By implementing the stream function and similarity variables (Kumar and Sood [19]):

$$\left.\begin{array}{l} \eta\;=\;\sqrt{\frac{U_e}{\nu x}}y,\quad\theta\left(\eta\right)=\frac{T-T_W}{T_w-T_\infty},\quad\phi\left(\eta\right)=\frac{C-C_W}{C_w-C_\infty},\\ \psi\;=\;\sqrt{a\nu}\;xf\left(\eta\right),\quad u=\frac{\partial\psi}{\partial y},\quad v=-\frac{\partial\psi}{\partial x}, \end{array}\right\},(7)$$

on equations (1) - (6), equation (1) is identically satisfied while equations (2) - (6) give

$$\left.\begin{array}{r} f'''+ff''-\left(f'\right)^2+1+B\left(1-f'\right)+\\ \lambda\,\theta\left(1+\lambda 1\,\theta\right)+\gamma\,\phi\left(1+\gamma 1\,\phi\right)=0, \end{array}\right\} \quad (8)$$

$$\left.\begin{array}{r} \theta''+Pr\left[f\theta'-f'\theta+Q\theta\right]+Nt\,\left(\theta'\right)^2+Nb\,\theta'\phi'\\ +Ec\;Pr\left(f''\right)^2+Pr\;Ec\;B\left(1-f'\right)^2=0, \end{array}\right\} \quad (9)$$

$$\phi''+S_c\left(f\phi'-f'\phi\right)+\frac{Nt}{Nb}\theta''=0, \quad (10)$$

with the following boundary conditions:

$$f'=Z, f=0,\;\theta=1,\phi=1,\;\;at\;\;\eta=0, \quad (11)$$

$$f'=1,\;\;\theta=0,\phi=0,\;\;as\;\;\eta\rightarrow\infty, \quad (12)$$

where

$$\left.\begin{array}{l} B=\frac{\nu}{ak},\;\;\lambda=\frac{Gr_t}{Re_t{}^2},Gr_t=\frac{g\beta_0\,(T-T_\infty)x^3}{\nu^2},\\ Re_t=\frac{xU_e}{\nu},\gamma=\frac{Gr_c}{Re_c{}^2},\;Gr_c=\frac{g\beta 2\,(C-C_\infty)x^3}{\nu^2},\\ P\,r=\frac{\nu}{a},\;Nb=\frac{\tau D_B}{\alpha}\,(C_w-C_\infty),\;Re_c=\frac{x\mathrm{U_e}}{\nu},\\ Q=\frac{Q1}{a\,\rho C_p},Ec=\frac{(ax)^2}{C_p(T_w-\mathrm{T}_\infty)},S_c=\frac{\nu}{D_B},\;K=\frac{k_1}{a},\\ Z=\frac{c}{a},\;\lambda 1=\frac{\beta_1}{\beta_0}\,(T_w-T_\infty),\;\gamma 1=\frac{\beta_3}{\beta_2}\,(C_w-C_\infty),\\ \tau=\frac{\rho c_p}{\rho c_f},\;\;Nt=\frac{\tau D_T}{\alpha\mathrm{T}_\infty}\,(T_w-T_\infty), \end{array}\right\}$$

The flow characteristics are of interest because of their various practical applications in many fields. These include the local Skin friction C_f, the local Nusselt number $N_u x$, and the local Sherwood number $S_h x$ defined as

$$C_f=\frac{\tau_w}{\rho U_e{}^2},\;Nu_x=\frac{x}{K_1\,\left(T_w-T_\infty\right)},\;Sh_x=\frac{xj_w}{\alpha\left(C_w-C_\infty\right)}, \quad (13)$$

$$\tau_w=\mu\left(\frac{\partial u}{\partial y}\right)_{y=0},\;q_w=-k_1\left(\frac{\partial T}{\partial y}\right)_{y=0}\;\text{and}\;j_w=-\alpha\left(\frac{\partial C}{\partial y}\right)_{y=0}. \quad (14)$$

Applying the non-dimensional similarity parameters in equation (7) on equation (14) yields;

$$C_f Re_x{}^{1/2}=f''\left(0\right),\frac{Nu_x}{Re_x{}^{-1/2}}=-\theta'\left(0\right),\frac{Sh_x}{Re_x{}^{-1/2}}=-\phi'(0). \quad (15)$$

3. Results and Discussion

The numerical solution of the reduced system of equations (8) to (12) is conducted using the collocation method, employing assumed Legendre polynomial as basis functions within the symbolic computation software MATHEMATICA 11.3. Previous studies have shown that this method offers enhanced efficiency and simplicity in solving both linear and non-linear problems. A comprehensive explanation of the method's application can be found in Oyekunle *et al.* [36, 37], where the impacts of relevant parameters on flow dynamics are thoroughly

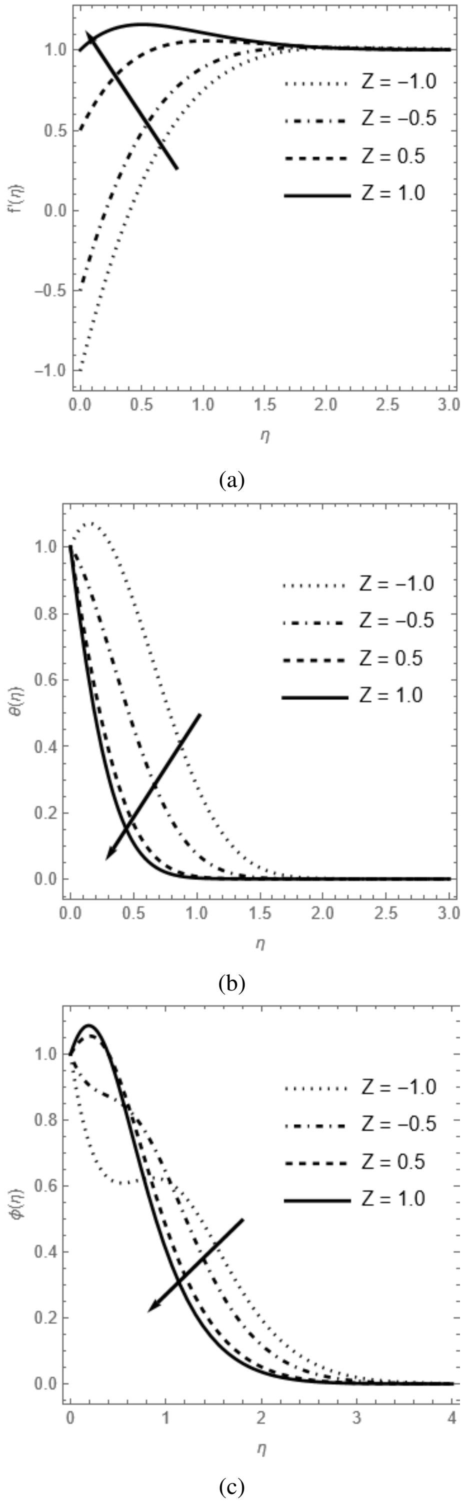

Figure 2: Impact of suction parameter (Z) on the flow distribution $f'(\eta)$, $\theta(\eta)$ and $\phi(\eta)$, respectively.

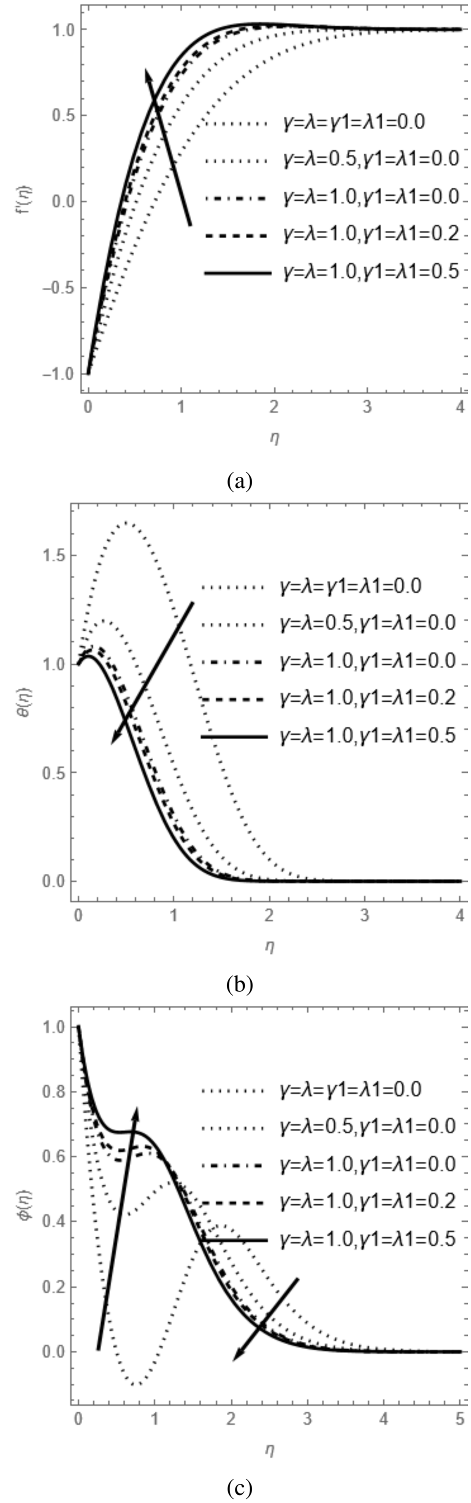

Figure 3: Impact of convection parameter (γ and λ) on the flow distribution $f'(\eta)$, $\theta(\eta)$ and $\phi(\eta)$, respectively.

explored. To ensure the validity of the obtained results, Table 1 present the comparison of the limited case of the current results with the results obtained in the work of Rakesh and Shilpa [35] and Wang [38]. The results obtained demonstrate a strong agreement with the conclusions presented in these earlier works, as depicted in the table below. Evaluating $f''(0)$ with respect to Z when $B = 0$, $Pr = 1$, $Nb = 0.01$, $Nt = 0.01$, $\lambda = 0$, $\lambda 1 = 0$, $\gamma = 0$ and $\gamma 1 = 0$ (see Table 1). This comparison confirmed the validity of the results, thereby strengthening the motivation to pursue the objectives outlined in this paper.

Table 1: Comparison of the present results and the work of Rakesh and Shilpa [35] and Wang [38].

Z	Present result	Rakesh and Shilpa [35]	Wang [38]
-0.25	1.40224	1.402253	1.40224
-0.50	1.49567	1.495685	1.49567
-0.75	1.4893	1.489316	1.48932
-1.00	1.32882	1.328840	1.32882
0.20	1.05113	1.0511379	1.051130
5.00	-10.2647	-10.26479	-10.26475

In this paper, rigorous computations were conducted to explore the effects of various parameters on the flow field. Graphs are provided to illustrate the influence of these parameters. Unless stated otherwise, the following parameter values are fixed to obtain the numerical results of this study: α = 0.5, Nt=0.1, λ1 = 0.5, β = 0.5, $B = 0.5$, λ = 1, $Sc = 1.0$, $Ec = 0.05$, $Nb = 0.1$, $Z = -1.0$, $Pr = 6.8$, and γ = 1. The dynamical response of the velocity ratio (Z) is depicted in Figure 2(a-c) for all the model profiles (velocity, temperature, and nanoparticle fraction). Physically, variations in this parameter (Z) alter the flow pressure distribution and enhance the fluid velocity at the solid boundary. Moreover, an increase in Z impacts the boundary layer thickness, thus intensifying fluid motion. As shown in Figures 2(a-c), the momentum distribution increases with the constant velocity ratio Z, leading to a lower temperature maintenance. Meanwhile, the nanoparticle volume fraction accelerates with Z up to a certain point along the channel width and then slows down. This indicates that the parameter Z has the capability to significantly enhance the nanoparticle volume fraction and momentum field along the stretching surface.

The dynamics of the Boussinesq approximation are described through both linear and nonlinear convection processes. The opposing forces due to gravity acceleration (Gr_t and Gr_c) characterize the behaviors of the linear and nonlinear convection terms λ, γ, $\lambda 1$, and $\gamma 1$, as profiled in Figure 3(a-c). Physically, the upright impact of flow geometry predicts a higher impact of gravity acceleration, while an inclined geometry tends to produce less impact from gravity. Additionally, setting g=0 in equation (2) results in the flow configuration becoming horizontal. The mathematical representation of the results in Figure 3(a-c) highlights that when $\lambda = \gamma = \lambda 1 = \gamma 1 = 0$, it represents a no-convection model; when $\lambda = 1 = \gamma$ and $\lambda 1 = \gamma 1 = 0$, it represents a linear convection model; and when $\lambda = 1 = \gamma$ and $\lambda 1 = \gamma 1 = 0.5$, it represents a nonlinear convection model. From the analysis, it is observed that an increase in the convection term signifies a rise in the momentum field, a reduction in energy distribution, and a pronounced enhancement in nanoparticle diffusion. An increase in nanoparticle diffusion suggests that nanoparticles are spreading more readily throughout the fluid medium. This could be significant in various applications involving nanoparticle transport, such as drug delivery, catalysis, or nanofluid-based heat transfer systems. Enhanced nanoparticle diffusion might affect the overall performance or efficiency of these processes.

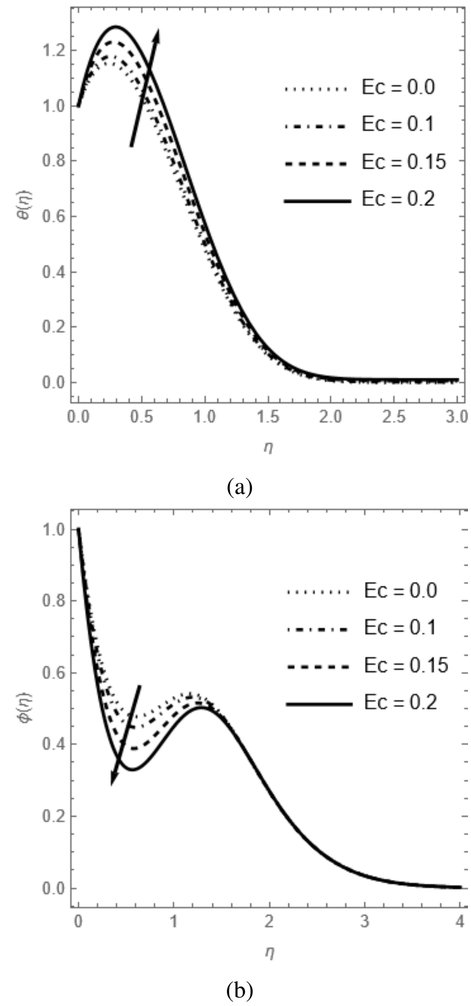

Figure 4: Impact of Eckert number (Ec) on the flow distribution $\theta(\eta)$ and $\phi(\eta)$, respectively.

The work done by the fluid on adjacent layers due to the action of shear forces is transformed into heat energy, also known as dissipation heat. This internal heat is measured by the dimensionless number Ec (Eckert number). The impact of Ec on energy and nanoparticle diffusion is displayed in Figures 4(a) and 4(b), respectively. A rise in the dimensionless number (Ec) enhances the energy and reduces the diffusion concentration of the nanoparticle volume fraction accordingly. These changes reflect the dynamic interplay between fluid flow characteristics, heat transfer processes, and nanoparticle dispersion within the system, and understanding these implications is crucial for optimizing various engineering applications, such as heat exchangers, nanofluid systems, or particle-laden flows. Similarly, the effect of the heat source term (Q) on temperature and concentration profiles is shown in Figures 5(a) and 5(b). We identify a continuous injection of heat energy into an accelerated temperature field, resulting in a decrease/less diffusion rate of the nanoparticle concentration due to heat absorption.

Figures 6(a-c) display the influence of the Darcy number (B) on the flow profiles. An increase in the Darcy number within a fluid flow system is associated with enhanced flow

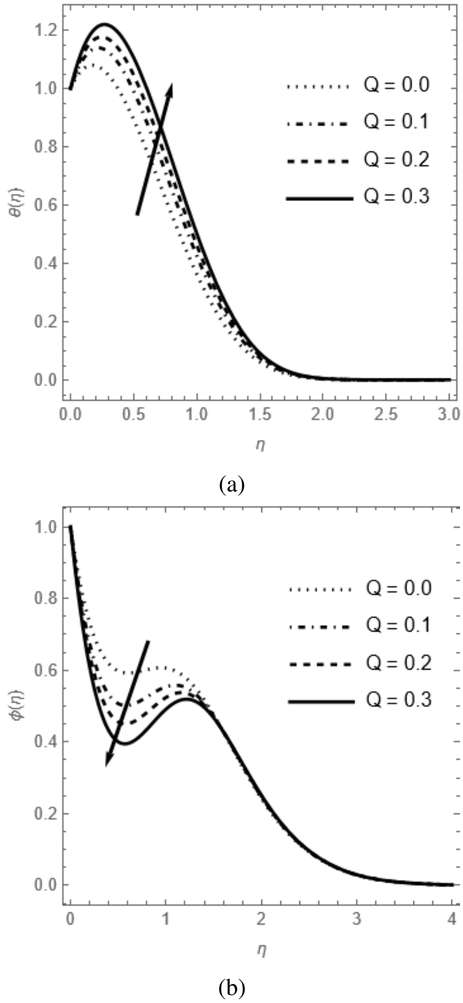

Figure 5: Impact of Heat generation parameter (Q) on the flow distribution $\theta(\eta)$ and $\phi(\eta)$, respectively.

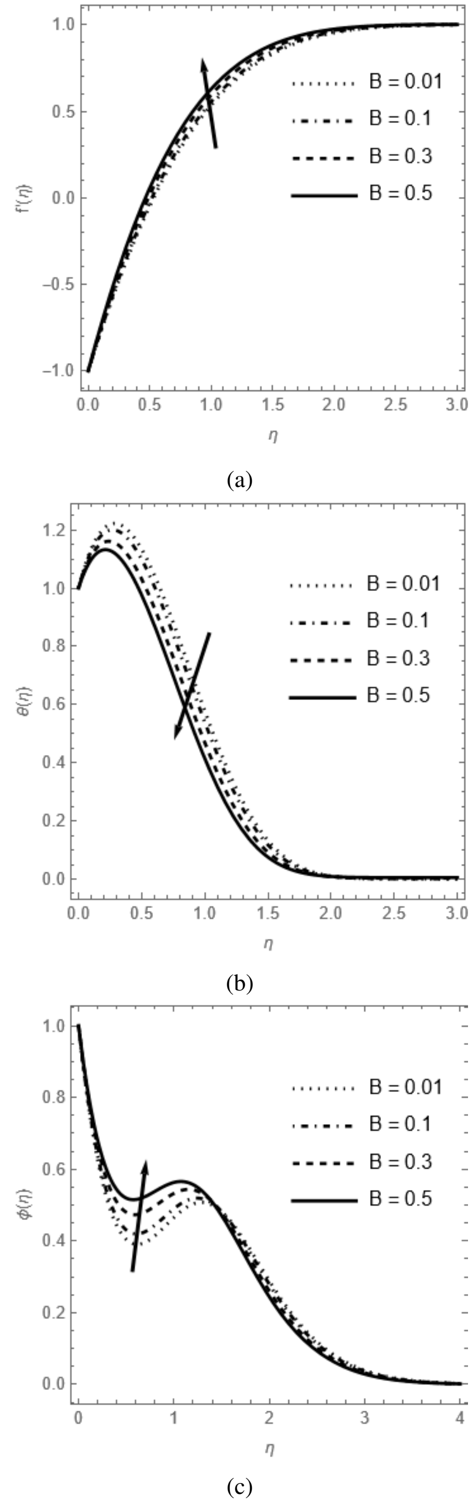

Figure 6: Impact of Darcy number (B) on the flow distribution $f'(\eta)$, $\theta(\eta)$ and $\phi(\eta)$, respectively.

velocity, decelerating temperature profiles, and non-uniform concentration distributions along the channel width. These changes reflect the complex interplay between flow dynamics, heat transfer processes, and mass transport phenomena within the system. Understanding these implications is essential for optimizing various engineering applications involving porous media flows, such as groundwater hydrology, petroleum reservoir engineering, or filtration processes. The thermophoresis parameter, Nt, resulting from the submersion of nanoparticles, increases liquid conductivity based on established theory. Therefore, Figure 7(a) shows an increase in velocity profile with the thermophoresis parameter Nt, while a decrease is observed in the temperature profile, as depicted in Figure 7(b).

With varying values of the dimensionless variables, Table 2 enumerates the skin friction coefficient ($f''(0)$), heat transfer coefficient ($\theta'(0)$) and mass transfer coefficient ($\phi'(0)$). A lower skin friction coefficient and increased heat transfer rate are indicated by the velocity ratio parameter (Z). As the internal heat generation parameter (Ec) is increased, skin friction, Nusselt number, and Sherwood number are enhanced. The Table further signified that skin friction and Nusselt number rise as a result of higher nonlinear thermal and solutal convection ratios, while Sherwood number decreases. Increasing Nt and Sc values result in reversed behavior of Z, $\lambda 1$ and $\beta 1$. Skin friction and Sherwood number increase with increases in B and Ec, while a decrease is observed with decreases in B and Ec.

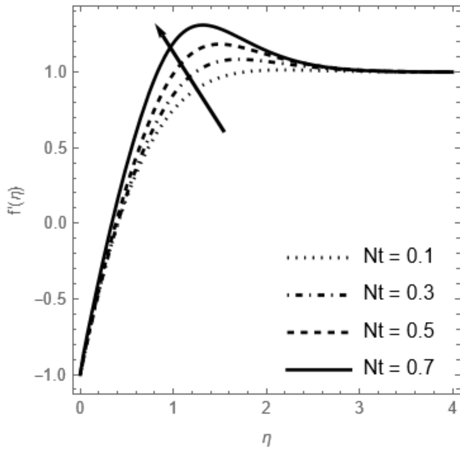

(a)

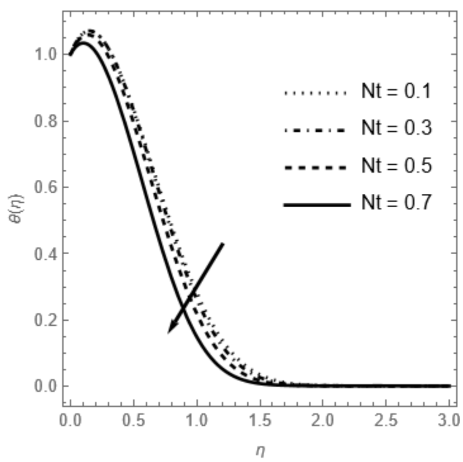

(b)

Figure 7: Impact of thermophoresis parameter (Nt) on the flow distribution $f'(\eta)$, $\theta(\eta)$, respectively.

4. Conclusion

The investigation of stagnation point flow of viscous nanofluid towards a shrinking sheet, considering various influential parameters, offers valuable insights into intricate fluid dynamics and thermal transport phenomena. Utilizing a similarity variable, the system is transformed into a solvable form. An approximate solution is then derived using the collocation method with Legendre polynomials as basis functions, revealing the dynamics of the involved physical variables. This scenario, which incorporates parameters such as suction parameter, convection parameter, Eckert number, heat generation, and Darcy number in porous media, provides a comprehensive understanding with numerous physical implications. However, the following key highlights:

- Velocity enhanced with an increase in Eckert and Darcy numbers, suction, convection, thermophoresis and heat generation parameters.
- Arise in Eckert and Darcy numbers, suction, convection, thermophoresis and heat generation parameters lead to a decrease in both energy and concentration distributions.
- Higher value of non-linear convection parameters give rise to skin friction and heat transfer coefficient.
- An increase in Darcy and Eckert numbers correspond to a decrease in heat transfer coefficient while skin friction and Sherwood number are increased.
- There is reduction in both skin friction, Nusselt and Sherwood numbers with an increase in thermophoresis number.

Understanding the interplay of these parameters in the stagnation point flow of viscous nanofluid towards a shrinking sheet provides a holistic view of the complex interactions between fluid dynamics, thermal transport, and material considerations. Balancing these parameters is crucial for optimizing heat and mass transfer processes while mitigating challenges associated with excessive velocities, turbulence, energy consumption, and material wear. This comprehensive analysis aids in designing efficient systems and processes across various engineering and industrial applications involving fluid dynamics and heat transfer.

NOMENCLATURE

α -Thermal diffusivity
g - Acceleration due to gravity
β_0, β_1 – Coefficients of thermal expansion

Table 2: Computational results of skin friction, Nusselt number and Sherwood number for variation of the embedding parameters when $Z = 0.5$, $Nt = 0.1$, $Nb = 0.1$, $Sc = 1.0$, $Da = 0.2$, $Pr = 6.8$, $Ec = 0.05$, $Q = 0.1$, $\lambda = 1$, $\gamma = 1$, $\lambda 1 = 0.5$, $\gamma 1 = 0.5$, $\beta 1 = 0.1$.

Dimensionless value		$f''(0)$	$\theta'(0)$	$\phi'(0)$
Z	-0.50	3.00860	0.09865	1.278110
	0.50	1.78785	2.38275	-0.374636
	1.00	0.95071	3.14256	-0.863024
B	0.01	3.36045	-1.67122	2.692220
	0.10	3.42734	-1.69686	2.726000
	0.30	3.55659	-1.76047	2.804410
Nt	0.10	3.36045	-1.67122	2.692220
	0.30	3.31229	-1.70940	7.277170
	0.50	3.31229	-1.70940	7.27717
Ec	0.10	3.41497	-2.76378	3.76642
	0.15	3.49367	-3.91642	4.90345
	0.20	3.59847	-5.16020	6.13334
Sc	0.50	3.47158	-1.62703	2.57771
	1.00	3.36045	-1.67122	2.69222
	1.50	3.31055	-1.69586	2.71437
$\gamma 1$	0.10	3.12614	-1.74125	2.72056
	0.30	3.24710	-1.70261	2.70394
	0.70	3.46780	-1.64530	2.68415
$\beta 1$	0.10	3.24190	-1.70316	2.69899
	0.30	3.30005	-1.68690	2.69525
	0.70	3.42286	-1.65619	2.68995

D_B – Brownian diffusion coefficients
B_0 – Applied magnetic field
τ – Ratio of the nano particles to the base fluid
u,v – Velocity components in the direction of x and y
K_1 – Chemical reaction coefficient
Q_1 – Heat source/ sink
Ec - Eckert number
μ – Viscosity
β_2, β_3– Coefficient of solutal expansion
ρ – Density
D_T – Thermophoresis diffusion coefficient
ν – Kinematic viscosity
T – Fluid temperature
C – Fluid concentration
K – Permeability constant
B – Permeability parameter
λ – Thermal linear parameter
λ1 – Thermal nonlinear parameter
Gr_t – Temperature Grashof numbers
Re_t – Temperature Reynoid number
γ – Solutal linear parameter
$\gamma 1$ – Solutal nonlinear parameter
Gr_c – Concentration Grashof number
Re_c – Concentration Reynold number
Pr – Prandtl number
N_B – Brownian motion parameter
N_T – Thermophoresis parameter
Q – Heat source/sink parameter
Sc – Schmidt number
K – Chemical reaction parameter
Z – Velocity ratio parameter

References

[1] S. Li, M. Faizan, F. Ali, G. Ramasekhar, T. Muhammad, H. A. E. W. Khalifa & Z. Ahmad, "Modelling and analysis of heat transfer in MHD stagnation point flow of Maxwell nanofluid over a porous rotating disk", Alexandria Engineering Journal **91** (2024) 237. https://doi.org/10.1016/j.aej.2024.02.002.

[2] Z. Mahmood, K. Rafique, U. Khan, M. Abd El-Rahman & R. Alharbi, "Analysis of mixed convective stagnation point flow of hybrid nanofluid over sheet with variable thermal conductivity and slip Conditions: A Model-Based study", International Journal of Heat and Fluid Flow **106** (2024) 109296. https://doi.org/10.1016/j.ijheatfluidflow.2024.109296.

[3] Y. O. Tijani, S. D. Oloniiju, M. O. Oni & M. T. Akolade, "Surface dynamics and thermophysical mechanics on Reiner–Philippoff fluid flow", International Journal of Modern Physics B (2023) 2450339. https://doi.org/10.1142/S0217979224503399.

[4] A. T. Brimmo & M. A. Qasaimeh, "Stagnation point flows in analytical chemistry and life sciences", RSC advances **7** (2017) 51206. https://doi.org/10.1039/C7RA11155J.

[5] N. S. Khashiie, N. Md Arifin & I. Pop, "Mixed convective stagnation point flow towards a vertical Riga plate in hybrid Cu-Al2O3/water nanofluid", Mathematics **8** (2020) 912. https://doi.org/10.3390/math8060912.

[6] O. D. Makinde, W. A. Khan & Z. H. Khan, "Stagnation point flow of MHD chemically reacting nanofluid over a stretching convective surface with slip and radiative heat", Proceedings of the Institution of Mechanical Engineers, Part E: Journal of Process Mechanical Engineering **231** (2017) 695. https://doi.org/10.1177/0954408916629506.

[7] A. Shahid, The effectiveness of mass transfer in the MHD Upper-Convected Maxwell fluid flow on a stretched porous sheet near stagnation point: a numerical investigation", Inventions **5** (2020) 64. https://doi.org/10.3390/inventions5040064.

[8] M. Zaheer, S. Z. Abbas, N. Huang & Y. Elmasry, "Analysis of buoyancy features on magneto hydrodynamic stagnation point flow of nanofluid using homotopy analysis method", International Journal of Heat and Mass Transfer **221** (2024) 125045. https://doi.org/10.1016/j.ijheatmasstransfer.2023.125045.

[9] G. Kenea & W. Ibrahim, "Nonlinear convection stagnation point flow of Oldroyd-B nanofluid with non-Fourier heat and non-Fick's mass flux over a spinning sphere", Scientific Reports **14** (2024) 841. https://doi.org/10.1038/s41598-024-51475-z.

[10] V. B. Awati, A. Goravar & M. Kumar, "Spectral and Haar wavelet collocation method for the solution of heat generation and viscous dissipation in micro-polar nanofluid for MHD stagnation point flow", Mathematics and Computers in Simulation **215** (2024) 158. https://doi.org/10.1016/j.matcom.2023.07.031.

[11] P. M. Patil & M. Kulkarni, "Nonlinear mixed convective nanofluid flow along moving vertical rough plate", Revista mexicana de física **66** (2020) 153. https://doi.org/10.31349/revmexfis.66.153.

[12] A. M. M. Raju, G. S. S. Raju & B. Mallikarjuna, "Unsteady quadratic convective flow of a rotating non-Newtonian fluid over a rotating cone in a porous medium", International Journal of Advanced Research in Computer Science **8** (2017) 6. https://doi.org/10.26483/ijarcs.v8i6.4474.

[13] A. B. Raju, G. S. S. Raju, B. Mallikarjuna & C. S. K. Raju, "Effect of nonlinear convection and variable properties on Darcy flow of non-Newtonian fluid over a rotating cone", International Journal of Research Engineering and Application Management **4** (2018) 586. https://doi.org/10.18231/2454-9150.2018.0270.

[14] S. A. Khan, T. Hayat, A. Alsaedi & B. Ahmad, "Heat and mass transfer enhancement in nonlinear mixed convective flow: Buongiorno model and melting heat phenomenon", International Communications in Heat and Mass Transfer **153** (2024) 107330. https://doi.org/10.1016/j.icheatmasstransfer.2024.107330.

[15] M. T. Akolade, "Numerical approach to second law analysis of a dissipative Carreau fluid dynamic over nonlinear stretching sheet", International Journal of Ambient Energy **44** (2023) 1427. https://doi.org/10.1080/01430750.2023.2175725.

[16] M. T. Akolade, T. L. Oyekunle, H. O. Momoh & M. M. Awad, "Thermophoretic movement, heat source, and sink influence on the Williamson fluid past a Riga surface with positive and negative Soret-Dufour mechanism", Heat Transfer **51** (2022) 4228. https://doi.org/10.1002/htj.22497.

[17] A. S. Idowu, M. T. Akolade, T. L. Oyekunle & J. U. Abubakar, "Nonlinear convection flow of dissipative Casson nanofluid through an inclined annular microchannel with a porous medium", Heat transfer **50** (2021) 3388. https://doi.org/10.1002/htj.22033.

[18] J. O. Olabode, A. S. Idowu, M. T. Akolade & E. O. Titiloye, "Unsteady flow analysis of Maxwell fluid with temperature dependent variable properties and quadratic thermo-solutal convection influence", Partial Differential Equations in Applied Mathematics. **4** (2021) 100078. https://doi.org/10.1016/j.padiff.2021.100078.

[19] R. Kumar & S. Sood, "Interaction of magnetic field and nonlinear convection in the stagnation point flow over a shrinking sheet", Journal of Engineering **2016** (2016) 6752520. https://doi.org/10.1155/2016/6752520.

[20] P. M. Patil & H. F. Shankar, "Double-diffusive nonlinear convection dusty fluid flow over a cone under the influence of activation energy", Indian Journal of Physics, **97** (2023) 2771. https://doi.org/10.1007/s12648-023-02657-4.

[21] A. Alam, D. N. K. Marwat & A. Ali, "Flow of nano-fluid over a sheet of variable thickness with non-uniform stretching (shrinking) and porous velocities", Advances in Mechanical Engineering **13** (2021) 1. https://doi.org/10.1177/16878140211012913.

[22] S. A. Agunbiade, A. A. Ayoade, T. L. Oyekunle & M. T. Akolade, "Brownian motion and thermophoresis influence in magnetized Maxwell upper-convected stagnation point fluid flow via a stretching porous surface", Journal of Taibah University for Science **18** (2024) 2301130. https://doi.org/10.1080/16583655.2023.2301130.

[23] V. Ramanjini, G. G.Krishna, M. Ramanuja, H. Kamala & S. R. Mishra, "Unsteady Prandtl nanofluidic flow through stretching sheet due to mixed convection, first-order slip, and chemical reaction", Journal of the Nigerian Society of Physical Sciences **5** (2023) 1140. https://doi.org/10.46481/jnsps.2023.1140.

[24] F. Deba, A. Rahman, Z. Khan, S. Iqbal & N. Sheikh, "Flow of a Williamson fluid over a stretching sheet containing nanoparticles", International Journal of system Engineering **5** (2021) 13. https://doi.org/10.11648/j.ijse.20210501.12.

[25] B. S. Goud, "Boundary layer and heat transfer Williamson fluid flow over a stretching sheet with Newtonian heating", Turkish Journal of Computer and Mathematics Education (TURCOMAT) **12** (2021) 1275.

[26] P. Lata, A. Kumar & A. Deepak, "Effect of magnetic field on thermosolutal convection in Jeffery Nanofluid with porous medium", Porous Media: An International Journal, **14** (2023) 17. https://doi.org/10.1615/SpecialTopicsRevPorousMedia.202346929.

[27] P. L. Sharma, A. Kumar & G. C. Rana, "Effect of magnetic field on thermosolutal convection in Jeffrey nanofluid with porous medium", Special Topics & Reviews in Porous Media: An International Journal **14** (2023) 17. https://doi.org/10.1615/SpecialTopicsRevPorousMedia.2023046929.

[28] P. L. Sharma, D. Bains & G. C. Rana, "Effect of variable gravity on thermal convection in Jeffrey nanofluid: Darcy-Brinkman model", Numerical Heat Transfer, Part B: Fundamentals **85** (2023) 776. https://doi.org/10.1080/10407790.2023.2256970.

[29] D. Yadav, J. Lee & H. H. Cho, "Throughflow and quadratic drag effects on the onset of convection in a Forchheimer-extended Darcy porous medium layer saturated by a nanofluid", Journal of the Brazilian Society of Mechanical Sciences and Engineering **38** (2016) 2299. https://doi.org/10.1007/s40430-016-0505-y

[30] D. Yadav, "Effect of electric field on the onset of Jeffery fluid convection in a heat-generating porous medium layer", Pramana **96** (2022) 19. https://doi.org/10.1007/s12043-021-02242-6.

[31] D. Yadav, M. Al-Siyabi, M. K. Awasthi, S. Al-Nadhairi, A. Al-Rahbi, M. Al-Subhi, R. Ragoju & K. Bhattacharyya, "Chemical reaction and internal heating effects on the double diffusive convection in porous membrane enclosures soaked with Maxwell fluid", Membranes **12** (2022) 338. https://doi.org/10.3390/membranes12030338.

[32] P. L. Sharma, M. Kapalta, A. Kumar, D. Bains, S. Gupta & P. Thakur, "Electrohy drodynamics convection in dielectric rotating Oldroydian nanofluid in porous medium". Journal of the Nigerian Society of Physical Sciences **5** (2023) 1231. https://doi.org/10.46481/jnsps.2023.1231.

[33] P. L. Sharma, D. Bains & P. Thakur, "Thermal instability of rotating Jeffrey nanofluids in porous media with variable gravity". Journal of the Nigerian Society of Physical Sciences **5** (2023) 1366. https://doi.org/10.46481/jnsps.2023.1366.

[34] N. Japili, H. Rosali & N. Bachok, "Suction effect on stagnation point flow and heat transfer over an exponentially shrinking sheet in a porous medium", Journal of Advanced Research in Fluid Mechanics and Thermal Sciences **73** (2020) 163. https://doi.org/10.37934/arfmts.73.2.163174.

[35] R. Kumar & S. Sood, "Interaction of magnetic field and nonlinear convection in the stagnation point flow over a shrinking sheet", Journal of Engineering **2016** (2016) 6752520. https://doi.org/10.1155/2016/6752520.

[36] T. L. Oyekunle, M. T. Akolade & S. A. Agunbiade, "Thermal-diffusion and Diffusion-thermo effects on heat and mass transfer in chemically reacting MHD Casson nanofluid with viscous dissipation", Applications and Applied Mathematics: An International Journal (AAM) **16** (2021) 39. https://digitalcommons.pvamu.edu/aam/vol16/iss1/39.

[37] T. L. Oyekunle, M. T. Akolade & S. A. Agunbiade, "The effect of thermophysical properties on nonlinear thermal-solutal convective flow of Casson nanofluid over an inclined surface with higher order chemical reaction", Journal of the Serbian Society for Computational Mechanics **16** (2022) 65. https://doi.org/10.24874/jsscm.2022.16.01.06.

[38] C. Y. Wang, "Stagnation flow towards a shrinking sheet", International Journal of Non-Linear Mechanics **43** (2008) 377. https://doi.org/10.1016/j.ijnonlinmec.2007.12.021.